Top Catal (2015) 58:1270–1275
DOI 10.1007/s11244-015-0496-4

ORIGINAL PAPER

Electrochemical Promotion of $Ir_{0.5}Pt_{0.5}O_2$/YSZ

S. Balomenou[1] · K. M. Papazisi[1] · D. Tsiplakides[1,2]

Abstract A high surface area, nanostructured bimetallic oxide catalyst, $Ir_{0.5}Pt_{0.5}O_2$, deposited on YSZ was studied for the electrochemical promotion of ethylene oxidation. The catalyst was synthesized using the modified Adams fusion method and was characterized regarding its structure, morphology and specific surface area via XPS, XRD, HRTEM, SEM and BET. Regarding the performance for electrochemical promotion, it was found that the rate of ethylene oxidation can be enhanced significantly and in a strongly non-faradaic manner via positive potential application, exhibiting strongly electrophobic behaviour.

Keywords Electrochemical promotion · EPOC · $Ir_{0.5}Pt_{0.5}O_2$ · Adams fusion method

1 Introduction

Electrochemical promotion of catalysis (EPOC) [1] takes place when small electrical potentials are applied to micro- or nano-dispersed catalysts supported on solid ceramic or polymeric electrolytes. The very small electrical currents (in the range of 10–1000 μA/cm^2) flowing through such structures, as a consequence of the applied potential, can cause dramatic (up to 1350-fold [2]) and reversible enhancement of catalytic activity, often accompanied by major improvements in selectivity. EPOC phenomenon has been observed for many reactions catalyzed by a variety of catalyst-support systems, and EPOC-induced enhancements of reaction rates were up to five orders of magnitude larger than those anticipated for purely electrolytic effects of the currents governed by Faraday's Law. Since the discovery of the phenomenon in 1981 [3] for the case of ethylene epoxidation on a Ag catalyst film deposited on YSZ, EPOC has been described in detail [1, 4] in practically all modern electrochemical and catalytic handbooks, and has proven to be a general phenomenon at the interface of catalysis and electrochemistry.

The discovery of EPOC opened exciting possibilities for electrically "tuning" (accelerating, directing or, if desired, slowing down) catalytic-chemical processes, but practical applications remain largely unexplored [5]. This is mainly because most of the published work in EPOC area has focused on low surface area catalysts with very low catalyst dispersion. However, there exist some exploratory works utilizing highly dispersed (commercial) catalysts, subjected to direct or even indirect polarisation, and sputtered films for electropromotion, which show very promising results [1, 4, 6–8].

The first EPOC studies with metal-type conducting metal oxides (e.g. IrO_2, RuO_2 and IrO_2-TiO_2 mixtures) were reported in the literature twenty years ago by Comninellis and his coworkers [9–14]. EPOC on conducting metal oxides revealed similar characteristics with metal electrocatalysts since they possess high density of states at the Fermi level and are, in this respect, very similar to metals. One of the most interesting and potentially important from a practical viewpoint aspect of electrochemical promotion on metal oxides is the "permanent NEMCA" behaviour, which refers to the phenomenon of permanent rate enhancement after a temporary potential

---

✉ D. Tsiplakides
dtsiplak@cperi.certh.gr

[1] Chemical Process and Energy Resources Institute/Centre for Research and Technology-Hellas, 6th km Charilaou-Thermi Rd, 57001 Thessaloniki, Greece

[2] Department of Chemistry, Aristotle University of Thessaloniki, 54124 Thessaloniki, Greece

treatment. Finally, the EPOC study of an IrO_2 oxide catalyst in contact with a mixed electronic-ionic conductor (TiO_2) provided an unambiguous proof of the complete equivalence of "classical" metal-support interaction utilizing TiO_2 and electrochemical promotion utilizing YSZ [15–18].

In the present work, a high surface area, nanostructured bimetallic oxide catalyst, $Ir_{0.5}Pt_{0.5}O_2$ was synthesized, casted as working electrode on YSZ and was studied for the electrochemical promotion of ethylene oxidation probe reaction.

2 Experimental

The $Ir_{0.5}Pt_{0.5}O_2$ nanoparticle catalyst was synthesized via a modified Adams fusion method [19, 20], using metal chloride precursors ($H_2IrCl_6 \cdot 6H_2O$ and $H_2PtCl_6 \cdot xH_2O$, Alfa Aesar), thermal treatment at 500 °C for 30 min and consequent washing/filtration with excess of DD water in order to remove all Cl^- ions.

The material was characterized regarding its physicochemical properties. Crystalline phase and structure were assessed using X-ray diffraction analysis. The morphology, particles size, and microstructure of the metal oxide were studied with electron microscopy (HR-TEM coupled with X-ray EDS and SEM). The specific surface area and pore volume of the catalyst were measured with BET. Finally, the surface composition and metal oxidation state were studied using X-ray photoelectron spectroscopy (XPS).

The synthesized metal oxide catalyst was casted on the surface of a YSZ disk (8 mol% Y_2O_3, thickness 1.6 ± 0.05 mm, diameter 20 mm, Dynamic Ceramic, Technox 802) in the form of a thin film. The catalyst layer was deposited by means of an ink consisting of 5 wt% catalyst, 43 wt% terpineol based ink vehicle (fuel cell materials) and ethanol. The catalyst ink was sonicated for 60 min to ensure uniform dispersion and consequently was applied on the YSZ surface. Then, the catalyst was calcined at 750 °C for 1 h. The formatted electrode had a geometric area of 1.55 cm^2. A gold counter electrode of similar geometric area was deposited on the opposite side of the YSZ pellet by applying a Metalor A1181 Au resinate and sintering at 850 °C for 30 min.

The sample was mounted in a button cell Probostat^{TM} test reactor. This SOFC type reactor operated at atmospheric pressure with gas flow rates up to 800 STP cm^3min^{-1}. A Princeton Applied Research potentiostat/galvanostat (Model 263A) was used for the application/measurement of potentials/currents. On-line monitoring of gas effluents was performed with a HORIBA VA-3000 infrared analyser.

3 Results and Discussion

3.1 Materials Characterization

The XRD powder diffraction pattern (Fig. 1) of the $Ir_{0.5}Pt_{0.5}O_2$ mixed oxide presents all the characteristic reflections of the Pt oxide with slightly different lattice parameters, while the two characteristic reflections at $2\theta = 34°$ and 40° have a broad shape, and are almost convoluted to a single wide peak as a result of the small particle size, also confirmed by the TEM analysis. The average crystallite size for the synthesized metal oxide was estimated to 2 nm, using the Scherrer equation, although for small (<5 nm) particle size materials the calculation is not considered to be quite accurate. The BET measurements revealed a high specific surface area of 270 m^2 gr^{-1}. This surface area value is among the highest reported in the literature for iridium based mono- or bi- metallic oxides. Evidently, the modified Adams fusion method is responsible for the high specific surface area obtained, and is directly related to the nano-scale particles formed.

Figure 2 shows HRTEM and SEM micrographs of the $Ir_{0.5}Pt_{0.5}O_2$ powder material before application on the YSZ support. The oxide consists of individual nanoparticles (with size ~2 nm) forming a porous microstructure interconnected in a network of conceivably higher electronic conductivity, as depicted in the SEM micrograph. In order to identify whether the nominal concentration of the bimetallic $Ir_{0.5}Pt_{0.5}O_2$ oxide was obtained, elemental mapping of the catalyst surface was performed with X-ray EDS analysis. The analysis revealed that a Ir:Pt ratio of 1 is achieved, also confirmed by XPS surface analysis (see below), a fact which indicates the effectiveness of the

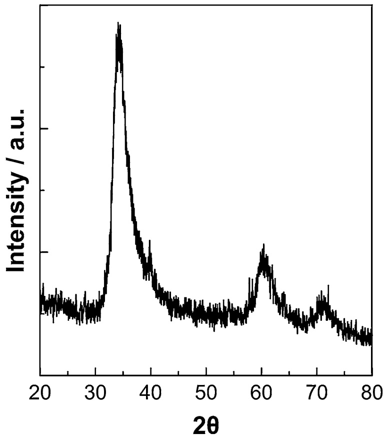

Fig. 1 X-ray diffraction (XRD) pattern of the $Ir_{0.5}Pt_{0.5}O_2$ mixed oxide

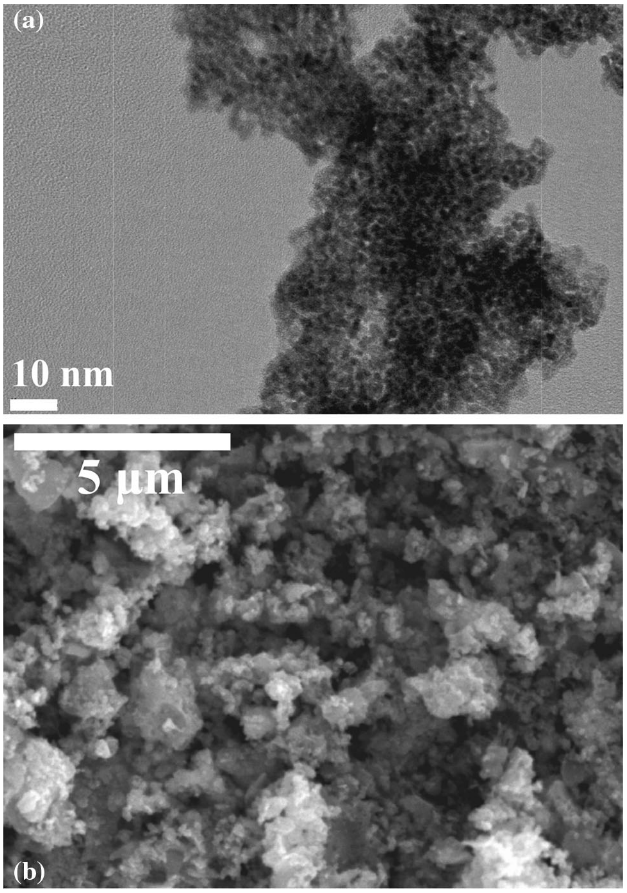

Fig. 2 **a** HRTEM and **b** SEM micrographs of the $Ir_{0.5}Pt_{0.5}O_2$ mixed oxide

synthesis method to result in mixed oxides of desired crystal structure (according to XRD) and concentration.

Figure 3a shows the Ir 4f and Pt 4f XPS core level spectra of the $Ir_{0.5}Pt_{0.5}O_2$ powder sample. The deconvolution of the Ir 4f spin orbit doublet gives a main Ir 4f component with Ir $4f_{7/2}$ binding energy (E_b) at 62.4 eV and Ir $4f_{5/2}$ at 65.1 eV (Fig. 3b). This is attributed to IrO_2 (Ir IV) [21, 22]. The spectrum appears to have a small contribution at higher binding energy (Ir $4f_{7/2}$ and Ir $4f_{5/2}$ at 63.8 and 66.7 eV, respectively), which is attributed to Ir at higher oxidation state [22], i.e. IrO_x with $x > 2$. The percentage of this component, attributed to the non-stoichiometric IrO_2 oxide, in the total Ir 4f spectrum is about 14 %. The fact that the majority of the surface Ir atoms in the mixed oxide exists in the tetravalent form (IrO_2) was also confirmed by calculating the Ir/O surface atomic ratio, using only the Ir 4f component at $E_b = 62.4$ eV and the O1s component at 530.5 eV. The Ir/O ratio was found to be close to 2. The Pt 4f spectrum consists of a doublet with the binding energies of Pt $4f_{7/2}$ and Pt $4f_{5/2}$ components at 74.7 and 77.9 eV, respectively, ($\Delta E_b = 3.2$ eV) which is typical for surface Pt atoms at valence +4, i.e. Pt(IV) or PtO_2 [23].

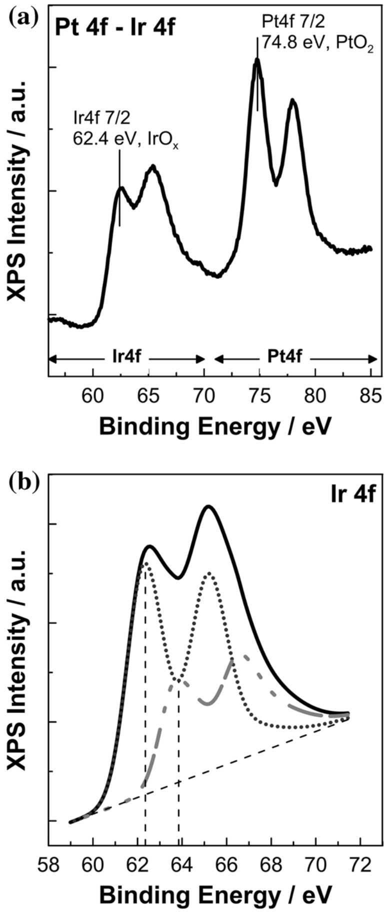

Fig. 3 **a** Ir 4f and Pt 4f XPS core level spectra and **b** deconvolution of the Ir 4f spectrum of the $Ir_{0.5}Pt_{0.5}O_2$ mixed oxide

Finally, the quantitative data processing of the Ir 4f and Pt 4f spectra leads to a Ir/Pt surface atomic stoichiometry Ir/Pt $\approx$ 0.98, which is in good agreement with the nominal value (50 % Ir–50 % Pt).

3.2 Electrochemical Promotion of Ethylene Oxidation

Ethylene oxidation as probe reaction was used to assess the potential of the synthesized electrocatalyst to induce EPOC. Figure 4 shows the effect of the applied potential (+2 V) on the transient catalytic rate at fixed composition of the gas phase (6 kPa O_2 and 0.85 kPa C_2H_4) at 300 °C. Before potential application the catalytic rate of carbon dioxide production (initial open circuit catalytic rate) is 1.26×10^{-7} mol O/s. After ~260 min of potential application the rate seems to approach towards a new steady-state value, which is at least 5 times higher than the initial open circuit catalytic rate. Specifically, the rate enhancement ratio ρ is calculated to be 5.4. The increase in the catalytic rate Δr ($=5.5 \times 10^{-7}$ mol O/s), is (Λ=) 13,750 times higher than the faradaic rate I/2F

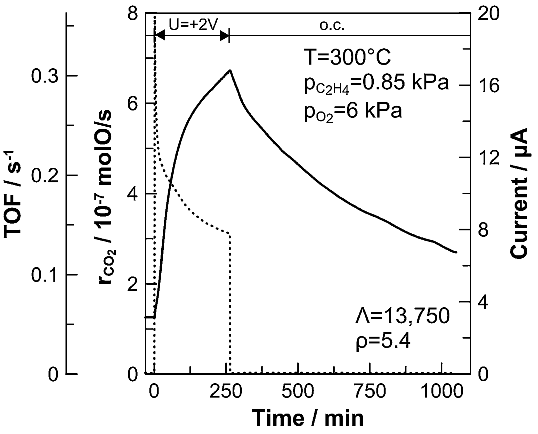

Fig. 4 Effect of applied potential (+2 V) on CO_2 production rate and turnover frequency, TOF, (*solid line*) and corresponding current response (*dashed line*). Conditions: 300 °C, 6 % O_2, 0.85 % C_2H_4

(=4 × 10^{-11} mol O/s). As shown in Fig. 4 upon current interruption the catalytic rate starts decreasing slowly, approaching a new open-circuit value, after more than 12 h, which is higher than its initial value, that is, before potential application. This behaviour ("permanent EPOC") has been previously reported [10] on IrO_2 studies of ethylene oxidation and has been attributed to the formation of $IrO_{2+\delta}$ at the IrO_2/YSZ interface and on the gas-exposed catalytic area during polarization (current or potential application). The catalytic activity of ethylene oxidation is considered to be higher on $Ir_{0.5}Pt_{0.5}O_{2+\delta}$ than on stoichiometric $Ir_{0.5}Pt_{0.5}O_2$, thus causing a permanent activation after potential pre-treatment or enrichment of the gas/catalyst interface with electrochemically pumped O^{2-}. After a short treatment with ethylene, in absence of oxygen, at the reaction temperature the open circuit rate was found to return to its initial value, i.e. before any current or potential application. This ethylene treatment procedure was followed in order to restore the initial state of the catalyst before performing any EPOC experiment.

The slow time response to potential application and interruption can be directly related to (a) the high surface area of the catalyst and (b) the slow reconstruction of catalyst surface and concomitant formation of higher oxide ($Ir_{0.5}Pt_{0.5}O_{2+\delta}$), which is expected to contribute on catalytic phenomena. It is worth noting that, although CO_2 was the only product observed under open circuit conditions, upon potential application the production of carbon monoxide was also observed; however, in ppm level (close to detection limit of the infrared analyser). The rate of CO production followed the same trend with CO_2 production, yet its value was more than an order of magnitude lower. The production of CO under similar conditions has never been reported in EPOC literature. An explanation on this observation cannot be given as further investigation needs to be conducted.

The corresponding catalyst surface area expressed in mol, N_G, can be approximated (after extrapolation to steady-state) via the rate time constant, τ, defined as the time required for the rate increase to reach 63 % of its final steady-state value upon constant current application [1]. The thus calculated N_G is 2.2 × 10^{-6} mol. This relatively high value, compared to typical EPOC electrodes prepared by the application of thin coatings of metal pastes, is in agreement with the high BET surface area of the present oxide powder which was the starting material for the catalyst ink. Based on this value, the TOF under open circuit conditions is 0.062 s^{-1} and equals 0.335 s^{-1} at anodic polarisation of +2 V (Fig. 4).

The catalytic rate dependence on oxygen to ethylene partial pressure ratio ($p_{O_2}/p_{C_2H_4}$) under both open-circuit and under positive (+2.5 V) applied potential is shown in Fig. 5. The rate exhibits a typical Langmuir–Hinshelwood behaviour with a maximum at high $p_{O_2}/p_{C_2H_4}$ equal to about 20. For low oxygen to ethylene ratios ($p_{O_2}/p_{C_2H_4}$) the rate is first order in O_2 while for high $p_{O_2}/p_{C_2H_4}$ ratios the rate becomes negative order in O_2. Thus, for low $p_{O_2}/p_{C_2H_4}$ ratios the catalyst surface is covered predominantly by C_2H_4 while at high ratios the catalyst surface is predominantly covered by O_2. It is interesting to note that the rate follows electrophobic behaviour (rate increases via positive potential application) over the whole range of $p_{O_2}/p_{C_2H_4}$ partial pressure ratios examined.

Almost all previous experimental studies on electrochemical promotion of ethylene oxidation on metal and metal oxide (e.g. IrO_2 and RuO_2) electrocatalysts [1] have assumed implicitly the Langmuir–Hinshelwood type catalytic mechanism involving as a rate limiting step the surface reactions between adsorbed hydrocarbon intermediates [24] and adsorbed atomic oxygen (O) originating from gaseous O_2 adsorption. Furthermore, these studies

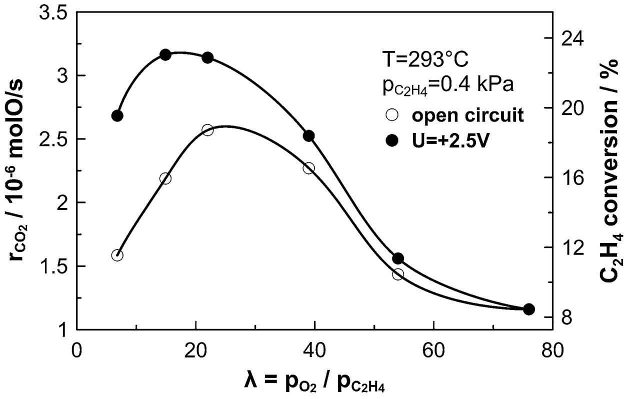

Fig. 5 Effect of oxygen to ethylene partial pressure ratio ($p_{O_2}/p_{C_2H_4}$) on CO_2 production rate under both open-circuit (*open symbols*) and under positive (*closed symbols*) applied potential (+2.5 V). Conditions: 293 °C, 0.4 % C_2H_4

have indicated weaker chemisorption of the electron donor (C_2H_4) than of the electron acceptor (O_2) on the catalyst surface. This behaviour has been rationalised by the application of the electrochemical promotion rules [25, 26]. In the case where the catalyst is a stable oxide, it was implicitly assumed that the oxide lattice oxygen does not participate in the catalytic reaction mechanism. Therefore, electrochemical promotion on stable oxides proceeds via the same mechanism as in the case of noble metal electrocatalysts interfaced with YSZ where the electrochemically supplied promoting backspillover oxygen species $O^{\delta-}$ migrate over the entire oxide catalyst/gas interface, thus establishing an effective double layer at the catalyst/gas interface [1, 17].

It should be mentioned that, although qualitative conclusions on the reaction mechanism may be extracted from the above kinetic behaviour, drawing quantitative conclusions should be avoided since the experiments were conducted under high (up to 23 %) C_2H_4 conversion (as depicted in the right vertical axis of Fig. 5). The choice of these experimental conditions was made in order to assess the potential of a high surface area and quite effective catalyst (TOFs are of the same order of magnitude with the corresponding ones for fully dispersed commercial catalysts) to exhibit electrochemical promotion. As a result, it was proven that electropromotion can be obtained under high reactants conversion (e.g. C_2H_4 conversion was enhanced from 16 to 23 %) with the effective rate enhancement ratio [27], ρ_c ($=\rho/\rho_{max}$, where ρ_{max} corresponds to near complete conversion of ethylene) ranging between 10 and 23 %; which is remarkably high for a single pellet reactor.

The corresponding faradaic efficiency, Λ, and rate enhancement ratio, ρ, values for the experimental conditions of Fig. 5 are shown in Fig. 6. Both Λ and ρ decrease rapidly as the oxygen to ethylene partial pressure ratio increases. The maximum values ($\Lambda_{max} = 7176$ and $\rho_{max} = 1.7$) were obtained at the lowest $p_{O_2}/p_{C_2H_4}$(=6.8) ratio employed. This ratio is still higher than the stoichiometric one, which according to the reaction stoichiometry is equal to 3. The observed behaviour is in agreement with the rationalisation of the catalytic reaction mechanism and the effect of a positive potential application on the chemisorptive bonds of both ethylene and oxygen, as described in detail above. Briefly, at low $p_{O_2}/p_{C_2H_4}$ the catalyst surface is partly covered by weakly adsorbed C_2H_4 (electron donor) molecules and oxygen (electron acceptor) atoms. The establishment of the effective double layer (M–$O^{\delta-}$, where M is the metal oxide) as well as the formation of higher oxide ($Ir_{0.5}Pt_{0.5}O_{2+\delta}$) via positive potential application leads to an increase of catalyst work function, Φ, and a concomitant increase of the chemisorptive bond strength of C_2H_4 atoms with the surface and a weakening of the oxygen-catalyst bond; thus, giving rise to electropromotion. As the oxygen partial pressure is increased to very high values, oxygen adsorption dominates the surface and the effect of potential and work function on reactants' bond strengths, and therefore on catalyst activity, diminishes.

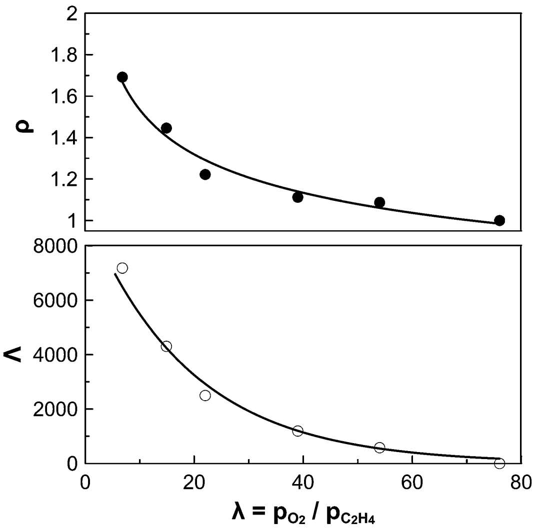

Fig. 6 Effect of oxygen to ethylene partial pressure ratio ($p_{O_2}/p_{C_2H_4}$) on faradaic efficiency, Λ, and rate enhancement ratio, ρ, values. Conditions as in Fig. 5

Mixed oxides have not received the same attention in the catalysis literature as the simple binary oxides have. The same applies also for the electrochemical promotion studies, where beside pure metal or metal oxide catalysts, only metal-oxide mixtures (e.g. Pd/CeO_2 or Ru/CeO_2) and binary oxide mixtures (e.g. IrO_2-TiO_2) have been utilised. The electropromotion in the aforementioned systems has been attributed to strong metal-support interaction caused by the promoting support action of the mixed ionic-electronic conductor (MIEC) oxide (CeO_2 or TiO_2) onto the catalyst (Pd, Ru or IrO_2). In the case of mixed oxides, one could only speculate that the catalytic activity and electropromotion is related to electronic factors (e.g. d-electron configuration/vacancies) in the solid solution formed. However, in order to support this hypothesis different oxide compositions should be explored and thus provide the basis for relating the systematic changes of activity with composition and electronic factors.

4 Conclusions

EPOC has been studied on $Ir_{0.5}Pt_{0.5}O_2$, a high surface area, nanostructured bimetallic oxide catalyst film deposited on YSZ for ethylene oxidation. Application of a positive potential (+2 V) induced non-faradaic enhancement in catalytic rate with rate enhancement ratio, ρ, and faradaic efficiency, Λ, values equal to 5.4 and 13,750, respectively, at 300 °C. The turnover frequencies for the electropromoted electrode surface were of the same order of magnitude with the corresponding ones for fully dispersed commercial catalysts.

Acknowledgments This work is co-financed by the EU-European Social Fund and the Greek Ministry of Education Lifelong learning and Religious Affairs—General Secretariat for Research and Technology, under the National Action: "Cooperation" (09SYN-42-729).

References

1. Vayenas CG, Bebelis S, Pliangos C, Brosda S, Tsiplakides D (2001) Electrochemical activation of catalysis: promotion, electrochemical promotion and metal-support interactions. Kluwer Academic/Plenum Publishers, New York
2. Kotsionopoulos N, Bebelis S (2005) Electrochemical promotion of the oxidation of propane on Pt/YSZ and Rh/YSZ catalyst-electrodes. J Appl Electrochem 35:1253–1264
3. Stoukides M, Vayenas CG (1981) The effect of electrochemical oxygen pumping on the rate and selectivity of ethylene oxidation on polycrystalline silver. J Catal 70:137–146
4. Vernoux P, Lizarraga L, Tsampas MN, Sapountzi FM, De Lucas-Consuegra A, Valverde J-L, Souentie S, Vayenas CG, Tsiplakides D, Balomenou S, Baranova EA (2013) Ionically conducting ceramics as active catalyst supports. Chem Rev 113(10): 8192–8260
5. Tsiplakides D, Balomenou S (2009) Milestones and perspectives in electrochemically promoted catalysis. Catal Today 146(3–4):312–318
6. Roche V, Revel R, Vernoux P (2010) Electrochemical promotion of YSZ monolith honeycomb for deep oxidation of methane. Catal Commun 11(13):1076–1080
7. Kambolis A, Lizarraga L, Tsampas MN, Burel L, Rieu M, Viricelle JP, Vernoux P (2012) Electrochemical promotion of catalysis with highly dispersed Pt nanoparticles. Electrochem Commun 19:5–8
8. Balomenou S, Tsiplakides D, Katsaounis A, Thiemann-Handler S, Cramer B, Foti G, Comninellis C, Vayenas CG (2004) Novel monolithic electrochemically promoted catalytic reactor for environmentally important reactions. Appl Catal B-Environ 52(3): 181–196
9. Varkaraki E, Nicole J, Plattner E, Comninellis C, Vayenas CG (1995) Electrochemical promotion of IrO_2 catalyst for the gas phase combustion of ethylene. J Appl Electrochem 25:978–981
10. Nicole J, Comninellis C (1998) Electrochemical promotion of IrO_2 catalyst activity for the gas phase combustion of ethylene. J Appl Electrochem 28:223–226
11. Tsiplakides D, Nicole J, Vayenas CG, Comninellis C (1998) Work function and catalytic activity measurements of an IrO_2 film deposited on YSZ subjected to in situ electrochemical promotion. J Electrochem Soc 145(3):905–908
12. Wodiunig S, Bokeloh F, Nicole J, Comninellis C (1999) Electrochemical promotion of RuO_2 catalyst dispersed on an yttria-stabilized zirconia monolith. Electrochem Solid St 2(6):281–283
13. Wodiunig S, Comninellis C (1999) Electrochemical promotion of RuO_2 catalysts for the gas phase combustion of C_2H_4. J Eur Ceram Soc 19:931–934
14. Constantinou I, Bolzonella I, Pliangos C, Comninellis C, Vayenas CG (2005) Electrochemical promotion of RuO_2 catalysts for the combustion of toluene and ethylene. Catal Lett 100(3–4):125–133
15. Nicole J, Tsiplakides D, Pliangos C, Verykios XE, Comninellis C, Vayenas CG (2001) Electrochemical promotion and metal-support interactions. J Catal 204:23–34
16. Vayenas CG, Archonta D, Tsiplakides D (2003) Scanning tunneling microscopy observation of the origin of electrochemical promotion and metal-support interactions. J Electroanal Chem 554:301–306
17. Vayenas CG, Brosda S, Pliangos C (2003) The double-layer approach to promotion, electrocatalysis, electrochemical promotion, and metal-support interactions. J Catal 216(1–2):487–504
18. Vayenas CG (2013) Promotion, electrochemical promotion and metal-support interactions: their common features. Catal Lett 143(11):1085–1097
19. Adams R, Shriner RL (1923) Platinum oxide as a catalyst in the reduction of organic compounds. III. Preparation and properties of the oxide of platinum obtained by the fusion of chloroplatinic acid with sodium nitrate. J Am Chem Soc 45:2171–2179
20. Papazisi KM, Siokou A, Balomenou S, Tsiplakides D (2012) Preparation and characterization of $Ir_xPt_{1-x}O_2$ anode electrocatalysts for the oxygen evolution reaction. Int J Hydrogen Energy 37:16642–16648
21. Yao S, Wang M, Madou M (2001) A pH electrode based on melt-oxidized iridium oxide. J Electrochem Soc 148(4):H29–H36
22. Chen RS, Chang HM, Huang YS, Tsai DS, Chattopadhyay S, Chen KH (2004) Growth and characterization of vertically aligned self-assembled IrO_2 nanotubes on oxide substrates. J Cryst Growth 271(1–2):105–112
23. Zhensheng J, Chanjuan X, Qingmei Z, Feng Y, Jiazheng Z, Jinzhen X (2003) Catalytic behavior of nanoparticle α-PtO_2 for ethanol oxidation. J Mol Catal A: Chem 191(1):61–66
24. Hegedus LL, Aris R, Bell AT, Boudart M, Chen NY, Gates BC, Haag WO, Somorjai GA, Wei J (1987) Catalyst design: progress and perspectives. Wiley, New York
25. Vayenas CG, Brosda S, Pliangos C (2001) Rules and mathematical modeling of electrochemical and chemical promotion: 1. Reaction classification and promotional rules. J Catal 203:329–350
26. Brosda S, Vayenas CG (2002) Rules and mathematical modeling of electrochemical and classical promotion. 2 Modeling. J Catal 208:38–53
27. Balomenou SP, Tsiplakides D, Katsaounis A, Brosda S, Hammad A, Foti G, Comninellis C, Thiemann-Handler S, Cramer B, Vayenas CG (2006) Monolithic electrochemically promoted reactors: a step for the practical utilization of electrochemical promotion. Solid State Ionics 177(26–32):2201–2204